(19) Europäisches Patentamt
European Patent Office
Office européen des brevets

(11) EP 1 094 330 A2

(12) EUROPEAN PATENT APPLICATION

(43) Date of publication:
25.04.2001 Bulletin 2001/17

(51) Int. Cl.[7]: **G01R 33/385**

(21) Application number: **00308446.4**

(22) Date of filing: **27.09.2000**

(84) Designated Contracting States:
AT BE CH CY DE DK ES FI FR GB GR IE IT LI LU MC NL PT SE
Designated Extension States:
AL LT LV MK RO SI

(30) Priority: **18.10.1999 US 419597**

(71) Applicant:
Marconi Medical Systems, Inc.
Cleveland, Ohio 44143 (US)

(72) Inventors:
- **Petropoulos, Labros S.**
  Solon, Ohio 44139 (US)
- **Schlitt, Heidi A.**
  Chesterland, Ohio 44026 (US)

(74) Representative: **Waters, Jeffrey**
Marconi Intellectual Property
Waterhouse Lane
Chelmsford Essex CM1 2QX (GB)

(54) Apparatus for magnetic resonance imaging and method of designing a gradient coil assembly

(57) A gradient coil assembly generates substantially linear magnetic gradients across the central portion of an examination region. The gradient coil assembly includes primary x, y, and z-gradient coils which generate a gradient magnetic field **(90)** having a non-zero first derivative in and adjacent the examination region. Preferably, the gradient coil assembly includes secondary, shielding x, y, and z coils which generate a magnetic field which substantially cancels, in an area outside a region defined by the shielding coils, a fringe magnetic field generated by the primary gradient coils. The existence of a non-zero first derivative in and adjacent the examination region eliminates aliasing effects attributable to the non-unique gradient field values on either side of a rollover point **(82)**. The non-unique values of the gradient magnetic field adjacent the rollover point caused structure near the rollover point to overlay each other. The unique non-linearity of the present gradient **(90)** adjacent the edges expands (magnifies) the image adjacent the edges. Because the expansion is unique, distortions at the edges are readily and accurately mapped back to linear.

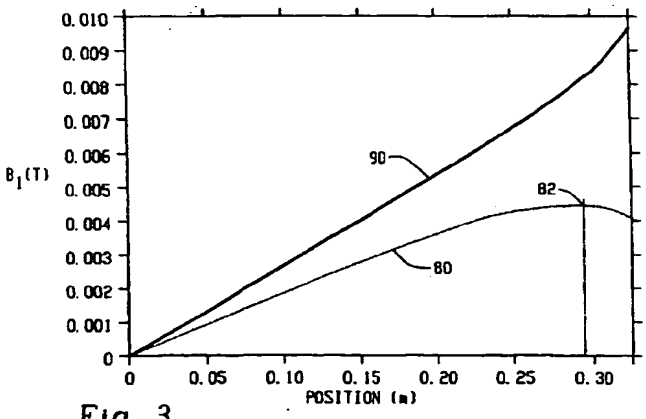

Fig. 3

EP 1 094 330 A2

BNSDOCID: <EP___1094330A2_I_>

Description

[0001] The present invention relates to the field of magnetic resonance imaging. It finds particular application in conjunction with gradient coils for a magnetic resonance imaging apparatus and will be described with particular reference thereto. However, it is to be appreciated that the present invention will also find application in conjunction with localized magnetic resonance spectroscopy systems and other applications which utilize gradient magnetic fields.

[0002] In magnetic resonance imaging, a uniform magnetic field is created through an examination region in which a subject to be examined is disposed. A series of radio frequency pulses and magnetic field gradients are applied to the examination region. Gradient fields are conventionally applied as a series of gradient pulses with pre-selected profiles. The radio frequency pulses excite magnetic resonance and the gradient field pulses phase and frequency encode the induced resonance. In this manner, phase and frequency encoded magnetic resonance signals are generated.

[0003] More specifically, the gradient magnetic field pulses are typically applied to select and encode the magnetic resonance with spatial position. In some embodiments, the magnetic field gradients are applied to select a slice or slab to be imaged. Ideally, the phase or frequency encoding uniquely identifies spatial location.

[0004] In bore type magnets, linear magnetic field gradients are commonly produced by cylindrical gradient field coils wound on and around a cylindrical former. Discrete coils are wound in a bunched or distributed fashion on a similar or larger diameter cylindrical tube, commonly 30-65 centimeters in diameter or larger.

[0005] Historically, gradient coil designs were developed in a "forward approach," whereby a set of initial coil positions were defined and the fields, energy, and inductance calculated. If these quantities were not within the particular design criteria, the coil positions were shifted (statistically or otherwise) and the results re-evaluated. This iterative procedure continued until a suitable design was obtained.

[0006] Recently, gradient coils are designed using the "inverse approach," whereby gradient fields are forced to match predetermined values at specified spatial locations inside the imaging volume. Then, a continuous current density is generated which is capable of producing such fields. This approach is adequate for designing non-shielded or actively shielded gradient coil sets.

[0007] Often, shielded gradient coil sets are designed such that their gradient magnetic field has an inherent rollover point along, but near the outer edge of its respective gradient axis. That is, the first derivative of the gradient magnetic field is zero at a certain location along the gradient axis and inside the physical volume bounded by the inner surface of the gradient structure. The gradient magnetic field takes on non-unique values after passing the rollover point where the first derivative of the gradient magnetic field is zero. The rollover point may be in the centre or near the edge of the bore, beyond where the subject is positioned. This design is problematic for an imaging sequence with a large field of view (FOV) in which portions of the subject are disposed between the rollover point and the bore. Areas of a subject that are located beyond the rollover point will alias back into the image, which causes ghosting and distortion of the image. A gradient deghosting and distortion algorithm is then implemented during postprocessing in order to compensate for distortions in the image. The gradient distortion algorithm, particularly when applied to all three gradient coils, extends the image postprocessing time and extends significantly the overall time of the magnetic resonance study.

[0008] In addition, information in the raw data related to the voxels located beyond the rollover point cannot be recovered uniquely. Voxels on either side of the rollover point that experience the same gradient strength are encoded indistinguishably. This limits the maximum FOV of a given sequence and limits the range of translational movement for the examined subject inside the image volume. This problem is particularly apparent when imaging extremities, such as shoulder, wrists, legs, and elbows, because typically these regions are located near the rollover point. Therefore, any attempt to move one side of an extremity near the isocentre of the imaging volume places the other side in the vicinity of the rollover point, which results in the aforementioned aliasing problems.

[0009] In accordance with one aspect of the present invention, a magnetic resonance imaging apparatus includes a main magnet for generating a main magnetic field through and surrounding an examination region. A gradient coil assembly generates gradient magnetic fields across the examination region. The gradient magnetic fields have a non-zero first derivative in and adjacent the examination region. An RF transmitter and coil assembly positioned adjacent the examination region excites magnetic resonance dipoles in and adjacent the examination region. An RF coil and receiver assembly receives and demodulates magnetic resonance signals from the resonating dipoles. A reconstruction processor reconstructs the demodulated magnetic resonance signals into an image representation.

[0010] In accordance with another aspect of the present invention, a method of designing a gradient coil assembly for a magnetic resonance imaging system includes selecting radius and length values for a primary gradient coil set and a secondary shielding coil set. The method further includes generating a first continuous current distribution for the primary gradient coil set. The first continuous current distribution is confined within predetermined finite geometric boundaries of a first surface defined above. The first continuous current distribution generates a gradient magnetic field across an examination region where the first derivative of the gradient magnetic field in and adjacent the examination region is non-zero. Further, a second continuous current distribution is generated for the secondary, shielding coil set. The sec-

BNSDOCID: <EP___1094330A2_I_>

ond continuous current distribution is confined within the predetermined finite geometric boundaries defined above. The first and second continuous current distributions generate a magnetic field which substantially cancels in an area outside the region defined by the secondary, shielding coil set. Next, the primary gradient coil set with the secondary, shielding coil set are optimized using an energy/inductance minimization algorithm. Finally, the primary gradient coil set and secondary, shielding coil set are discretized.

[0011] One advantage of the present invention is that it reduces or eliminates aliasing effects for magnetic resonance sequences with large fields of view.

[0012] Another advantage of the present invention is that it reduces or minimizes the need for a distortion correction algorithm.

[0013] Another advantage of the present invention is that it makes it possible to reduce postprocessing time for a magnetic resonance image.

[0014] Another advantage of the present invention is that it makes it possible to reduce overall time for a magnetic resonance study.

[0015] Yet another advantage of the present invention is that it makes it possible to increase the effective imaging volume.

[0016] Ways of carrying out the invention will now be described in detail, by way of example, with reference to the accompanying drawings, in which:

FIGURE 1 is a diagrammatic illustration of a magnetic resonance imaging system in accordance with the present invention;

FIGURE 2A is a diagrammatic illustration of a cross-section of the gradient coil assembly in accordance with the present invention;

FIGURE 2B is a perspective view of a primary gradient coil set in accordance with the present invention;

FIGURE 3 is an exemplary plot of transverse and longitudinal gradient magnetic field (B_1) vs. spatial position for a gradient coil with an inherent rollover point and a gradient coil without an inherent rollover point in accordance with the present invention;

FIGURE 4 is a flow chart for designing a shielded gradient coil assembly with a non-zero first derivative of the gradient magnetic field in accordance with the present invention;

FIGURES 5A and 5B are diagrammatic illustrations of one quadrant of an exemplary primary x-gradient coil and secondary shielding coil in accordance with the present invention;

FIGURES 6A and 6B are diagrammatic illustrations of one quadrant of an exemplary primary y-gradient coil and secondary shielding coil in accordance with the present invention;

FIGURE 7A is a distortion grid for a transverse slice through the z = 0.0 plane for an exemplary gradient coil set with no rollover point in accordance with the present invention;

FIGURE 7B is a distortion grid for a transverse slice through the z = 0.0 plane for an exemplary gradient coil set with an inherent rollover point in accordance with the prior art;

FIGURE 8A is a coronal distortion grid for an exemplary gradient coil set with no rollover point in accordance with the present invention; and

FIGURE 8B is a coronal distortion grid an exemplary gradient coil set with an inherent rollover point in accordance with the prior art.

[0017] With reference to FIGURE 1, a main magnetic field control **10** controls superconducting or resistive magnets **12** such that a substantially uniform, temporally constant main magnetic field is created along a z axis through an examination region **14**. Although a bore-type magnet is illustrated in FIGURE 1, it is to be appreciated that the present invention is equally applicable to open magnetic systems with vertically directed fields. A couch (not illustrated) suspends a subject to be examined within the examination region **14**. A magnetic resonance echo means applies a series of radio frequency (RF) and magnetic field gradient pulses to invert or excite magnetic spins, induce magnetic resonance, refocus magnetic resonance, manipulate magnetic resonance, spatially and otherwise encode the magnetic resonance, to

BNSDOCID: <EP___1094330A2_I_>

saturate spins, and the like to generate magnetic resonance imaging and spectroscopy sequences. More specifically, gradient pulse amplifiers **20** apply current pulses to a gradient coil assembly **22** that includes pairs of primary gradient coil assemblies **22a** and shield gradient coil assemblies **22b** with no roll-over point to create magnetic field gradients along x, y, and z axes of the examination region **14** with zero or minimal fringe fields outside of the bore. A digital radio frequency transmitter **24** transmits radio frequency pulses or pulse packets to a whole-body RF coil **26** to transmit RF pulses into the examination region **14**. A typical radio frequency pulse is composed of a packet of immediately contiguous pulse segments of short duration which, taken together with each other and any applied gradients, achieve a selected magnetic resonance manipulation. For whole-body applications, the resonance signals are commonly picked up by the whole-body RF coil **26**, but may be picked up by other specialized RF coils.

[0018] For generating images of local regions of the subject, specialized radio frequency coils are placed contiguous to the selected region. For example, an insertable RF coil may be inserted surrounding a selected region at the isocentre of the bore. The insertable RF coil is used to excite magnetic resonance and receive magnetic resonance signals emitting from the patient in the region being examined. Alternatively, the insertable RF coil can be used only to receive resonance signals introduced by whole-body RF coil transmissions. The resultant radio frequency signals are picked up by the whole-body RF coil **26**, the insertable RF coil, or other specialized RF coils and demodulated by a receiver **30**, preferably a digital receiver.

[0019] A sequence control circuit **40** controls the gradient pulse amplifiers **20** and the transmitter **24** to generate any of a plurality of multiple echo sequences such as echo planar imaging, echo volume imaging, gradient and spin echo imaging, fast spin echo imaging, and the like. For the selected sequence, the receiver **30** receives a plurality of data lines in rapid succession following each RF excitation pulse. Ultimately, the radio frequency signals received are demodulated and reconstructed into an image representation by a reconstruction processor **50** which applies a two-dimensional Fourier transform or other appropriate reconstruction algorithm. The image is then stored in an image memory **54**. As explained below, the resultant image adjacent its edges tends to be distorted (stretched or contracted). An image linearity correction processor **52** corrects the non-linearity. For example, the gradient field distortion can be empirically measured (see below) and the image can be mapped with the inverse of the mapped field distortion. Other distortion correction algorithms, as are known in the art, can also be utilized. Optionally, the distortion correction can be made in Fourier space prior to reconstruction, incorporated into the reconstruction algorithm, or downstream from the image memory. A human-readable display **56**, such as a video monitor, provides a human-readable display of the resultant image. The image may represent a planar slice through the patient, an array of parallel planar slices, a three-dimensional volume, or the like.

[0020] With reference to FIGURES 2A and 2B and continuing reference to FIGURE 1, the primary gradient coil assembly **22a** includes an inner dielectric former **60** of radius a. The inner former **60** defines the examination region **14** for receiving a portion of the subject to be examined. Y-gradient coils $\mathbf{62_1}$, $\mathbf{62_3}$, of a pattern determined by the below-referenced design procedure are laminated to the cylindrical surface of the inner former **60**. More specifically, for the y-gradient coil, the quadrant winding $\mathbf{62_1}$ of FIGURE 6A is connected with a like quadrant winding $\mathbf{62_3}$ along edge $\mathbf{62_m}$. The pair of winding assemblies $\mathbf{62_1}$, $\mathbf{62_3}$ are laminated with the edge **64** at the longitudinal centre of the former **60** and extending peripherally therearound. The x-gradient coils are mounted to the former **60** but 90 degrees rotated relative to the y-gradient coils. The x and y-gradient coils are electrically insulated from each other and preferably potted in an epoxy. The windings are preferably manufactured from a relatively thin conductive sheet, such as copper. The sheet is preferably cut before lamination to the former by water jet cutting, laser cutting, etching, or the like, and then bonded to a thin insulating substrate, minimizing radial thickness.

[0021] A primary z-gradient coil is also constructed of a conductive material, such as foil or wire. The primary z-gradient coil is preferably wound into grooves in the inner former **60** and potted in an epoxy. The secondary gradient coil assembly **22b** also includes an outer dielectric former **70** of radius b. The secondary x, y, and z shielding coils (not shown) are laminated into the cylindrical surface of the outer former **70** or on longitudinal rods, known as "combs," analogous to the primary gradient coils. These shielding coils are designed to cooperate with the primary gradient coils to generate a magnetic field which has a substantially zero magnetic flux density outside an area defined by the outer former.

[0022] With reference to FIGURE 3, prior art gradient coils sets typically are designed such that their gradient magnetic field profile **80** has an inherent rollover point **82** along, but near the edge of its respective axis, as shown. At the rollover point, the first derivative of the gradient magnetic field is zero. After passing the rollover point, where the first derivative is zero, the gradient field takes on non-unique values, i.e., assumes identical values to the gradient field on both sides of the rollover point. This leads to aliasing. When portions of the subject are disposed between the rollover point and the bore, areas of the subject that are located beyond the rollover point will alias back into the image, which causes ghosting of the image. Signals from two planes near the edge that are subject to the same gradient field strength are indistinguishable and are combined. In this manner, a ghost of the material beyond the rollover point is folded back on the material inside the rollover point.

[0023] In contrast, the present gradient coil assembly has a flux density **90** that possesses no such rollover point

BNSDOCID: <EP___1094330A2_I_>

within the physical volume bounded by the inner former, as shown in FIGURE 3. By designing the x, y, and z-gradient coils such that the first derivative of the gradient magnetic field (gradient field vector) in and adjacent to the examination region is non-zero, i.e., there is no rollover point, the above-discussed aliasing problems are minimized. Because there is no rollover point on the graph of gradient magnetic field versus position, all data values are unique. The non-zero first derivative gradient coil design presents regions on the gradient magnetic field vs. position curve **90** which typically increase non-linearity adjacent the edge region. For a reconstruction algorithm that assumes a linear gradient field, the edge regions are stretched in the reconstruction process. The non-linearity of the field is mapped, and the map is loaded into the linearity correction processor **52** to reverse the distortion. When the correction processor is before the reconstruction processor, it maps the actual gradient field back to linear and when it is after the reconstruction processor, it maps the stretched edges of the image back to normal.

[0024] The theoretical development, the design procedure and the numerical results for an exemplary shielded gradient coil with no rollover point of the gradient magnetic field along its perspective axis and inside the physical boundaries defined by the inner surface of the gradient tube is now discussed. Specifically, the theoretical development, the design, and the results of a gradient coil where the z component of the magnetic field varies linearly along the transverse direction (x, y-gradient coil), as well as, the axial gradient coil (z-gradient coil) will be presented. The x-gradient coil will be presented in its entirety as a representative for the transverse coils.

[0025] The flow chart for designing such a gradient coil structure is shown in FIGURE 4. Initially, a geometric configurations of the primary gradient coil step **100** sets the primary coil configuration and a secondary shielding coil configuration step **102** sets the secondary coil configuration. Namely, radius and length for each coil set are chosen. Next, an energy/inductance minimization step **104** optimizes the primary gradient coil set. As a result of the minimization process **104**, a first continuous current distribution generation step **106** generates the current distribution for the primary gradient coil set. The first continuous current distribution is confined to the geometric boundaries defined in step **100**. The first current distribution is selected such that it generates a magnetic gradient field across the examination region where the first derivative of the gradient magnetic field in and around the examination region is non-zero. Following this step, a second continuous current distribution selection step **108** generates the current distribution for the secondary, shielding coil set such that the second continuous current distribution is confined to the geometric boundaries defined in step **102**. The second continuous current distribution generates a magnetic field which, when combined with the magnetic field from the first current distribution, generates a substantially zero fringe magnetic field outside the secondary coil.

[0026] Further, in a current discretization step **110**, the continuous current distribution of the primary gradient coil set and the secondary, shielding coil set are discretized to generate the number of turns which is required for each coil within each coil set. Optionally, a verifying step **112** applies the Biot-Savart law to the discrete current pattern to verify its validity. Finally, in a measuring and mapping step **114**, non-linearities present in the gradient magnetic field near the edges of the examination region are measured and mapped back in order to correct the image near the edges.

[0027] The theoretical development of the energy optimization algorithm step **104** is discussed for both the transverse and the axial gradient coil.

[0028] The design of a finite, shielded transverse x-gradient coil involves the design of the primary coil (the coil closest to the subject) based on the inverse approach methodology. For the exemplary transverse coil the gradient magnetic field is anti-symmetric in the x direction around the geometric centre of the coil, while it is symmetric along the y and z directions. To generate such a field, the analytical expression of the current for the primary coil $J^a(r)$ can be written as:

$$\vec{J}^a(\vec{r})=[j_\varphi^a(\varphi,z)]\hat{a}_\varphi+j_z^a(\varphi,z)\hat{a}_z]\delta(\rho-a) \tag{1}$$

where $\delta(\rho-a)$ is the restriction that the current is confined to a cylindrical surface with radius a. The restriction to inner coil length, the confinement of the current density on the cylindrical surface, the azimuthal and axial symmetries for the j_φ^a and j_z^a and the constraint that the current density obeys the continuity equation provides the Fourier series expansion for both components around the geometric centre of the coil as follows:

$$j_\varphi^a(\varphi,z)=\cos(\varphi)\sum_{n=1}^{\infty} j_{\varphi n}^a \cos(k_n z) \qquad \text{for} \qquad |z|\leq\frac{L_a}{2} \tag{2}$$

BNSDOCID: <EP___1094330A2_I_>

$$j_z^a(\varphi, z) = \sin(\varphi) \sum_{n=1}^{\infty} \frac{-j_{\varphi_n}^a}{k_n a} \sin(k_n z) \qquad for \qquad |z| \le \frac{L_a}{2} \qquad (3)$$

where $j^a_{\varphi n}$ are the Fourier coefficients, L_a represents the total length of the inner coil, and $k_n=(2n\pi)/L_a$ since the current does not flow off the ends of the cylinder. Furthermore, both current components are zero for $|z|>L_a/2$.

[0029] In order minimize the fringe field of the primary coil in the area which is outside both the primary and the shielding coils, the Fourier transform of the current for the shielding coil satisfies the following relationship:

$$j_\varphi^b(\pm 1, k) = -\frac{aI_1'(ka)}{bI_1'(kb)} j_\varphi^a(\pm 1, k) \qquad (4)$$

with

$$j_\varphi^a(\pm 1, k) = \frac{L_a}{4} \sum_{n=1}^{\infty} j_{\varphi_n}^a \psi_n(k)$$

$$\psi_n(k) = \left[\frac{\sin(k-k_n)\frac{L_a}{2}}{(k-k_n)\frac{L_a}{2}} + \frac{\sin(k+k_n)\frac{L_a}{2}}{(k+k_n)\frac{L_a}{2}} \right] \qquad (5)$$

where I'_m, K'_m represent the derivatives with respect to the argument of the modified Bessel functions of the first and the second kind.

[0030] In this case, the expression for the z component of the magnetic field in the area inside both coils can be written as:

$$B_z = -\frac{\mu_0 a L_a}{4\pi} \cos(\varphi) \sum_{n=1}^{\infty} j_{\varphi_n}^a \int_0^{+\infty} dk \; k \; \cos(kz) \psi_n(k) I_1(k\rho) K_1'(ka) \left[1 - \frac{I_1'(ka) K_1'(kb)}{I_1'(kb) K_1'(ka)} \right] \qquad (6)$$

[0031] Furthermore, the expression for the stored magnetic energy can also be written as:

BNSDOCID: <EP___1094330A2_I_>

$$W=$$

$$-\frac{\mu_0 a^2 L_a^2}{16}\sum_{n=1}^{\infty}\sum_{n'=1}^{\infty} j^a_{\varphi_n} j^a_{\varphi'_n} \int_0^{+\infty} dk\ \psi_n(k)\psi_{n'}(k)\, I_1'(ka)\, K_1'(ka)$$

$$\left[1-\frac{I_1'(ka)\,K_1'(kb)}{I_1'(kb)\,K_1'(ka)}\right] \qquad (7)$$

[0032] As a next step, the functional ε is constructed in terms of W and B_z as:

$$\varepsilon\left(j^a_{\varphi_n}\right) = W - \sum_{j=1}^{N} \lambda_j \left(B_z(\vec{r}_j) - B_{zSC}(\vec{r}_j)\right) \qquad (7a)$$

where λ_j are the Lagrange multipliers and B_{zSC} represents the constraint values of the z component of the magnetic field at the specified N points. Minimizing ε, a quadratic function of the current, with respect to the current coefficients $j^a_{\varphi n}$ results in a matrix equation for $j^a_{\varphi n}$ as:

$$\sum_{n'=1}^{\infty} j^a_{\varphi'_n} \frac{aL_a\Pi}{2} \int_0^{+\infty} dk \psi_n(k)\psi_{n'}(k)\, I_1'(ka)\, K_1'(ka) \left[1-\frac{I_1'(ka)\,K_1'(kb)}{I_1'(kb)\,K_1'(ka)}\right] =$$

$$\sum_{j=1}^{N} \cos(\varphi_j) \int_0^{+\infty} dk\ k\ \cos(kz_j)\psi_n(k)\, I_1(k\rho_j)\, K_1'(ka)$$

$$\left[1-\frac{I_1'(ka)\,K_1'(kb)}{I_1'(kb)\,K_1'(ka)}\right] \qquad (8),$$

where the evaluation of the Lagrange multipliers λ_j can be done via the constraint equation.

[0033] By truncating the previous infinite summations at M terms, and using compact notation, the previous expression is modified to read:

$$\sum_{n'=1}^{M} j^a_{\varphi'_n} C_{n',n} = \sum_{j=1}^{N} \lambda_j D_{jn} \qquad (9)$$

or in matrix form:

$$J^a\, C = \lambda\, D \Rightarrow J^a = \lambda D C^{-1} \qquad (10)$$

but

$$B_z = J^a D^t \Rightarrow B_z = \lambda D C^{-1} D^t \qquad (11)$$

which leads to

BNSDOCID: <EP__1094330A2_I_>

$$\lambda = B_z[DC^{-1}D^t]^{-1} \Rightarrow J^a = B_z[DC^{-1}D^t]^{-1}DC^{-1} \quad (12).$$

[0034] Inverting the previous matrix equation, a solution for $j^a_{\varphi n}$, and hence for the current density, is obtained. When the continuous current distribution for both the primary and shield coils is evaluated, the stream function technique is used to discretize the current density for both primary and shield coils in such a way that the absolute integer number of turns is obtained for both coils for a given common current value per loop. The discretization and the magnetic gradient field inside the desired imaging volume are then calculated proceeding with steps 6 through 8 of Figure 4.

[0035] For the design of the exemplary primary x-gradient coil, the radius of the cylinder for the primary coil is set equal to 0.3438500 m and its total length is restricted to 1.066400 m. In addition, the radius of the secondary coil is equal to 0.435224 m. The constraints for the design of the primary coil are shown in Table 1. The constraints for the primary y-gradient coil are shown in Table 2.

n	ρ_i	z_i	$B_{zsc}(T)$
1	0.001	0.000	0.000027000
2	0.230	0.000	0.006211244
3	0.001	0.200	0.000021600

Table 1:Constraint set used for the design for the x-gradient coil.

Values for ρ and z are in m, values for $B_{zsc}(T)$ are in Tesla.

[0036] As shown in Table 1, the first constraint point defines a gradient strength for the first primary and single shield coil to be 27.0 mT/m, the second constraint point specifies a +0.1% linearity of the gradient field along the gradient (x) axis and up to the distance of 23.0 cm for the isocentre of the gradient field, while the third constraint point specifies a -20% uniformity of the gradient field inside the 40 cm imaging volume.

n	ρ_i	z_i	$B_{zsc}(T)$
1	0.001	0.000	0.000027000
2	0.265	0.000	0.007870500
3	0.001	0.200	0.0000217800

Table 2: Constraint set used for the design for the y-gradient coil.

Values for ρ and z are in m, values for $B_{zsc}(T)$ are in Tesla.

[0037] For the exemplary y-gradient shielded coil, the radius of the primary coil is a = 0.336040m with a length of 1.0534m, while the radius of the secondary coil is b = 0.431414m. As shown in Table 2, the first constraint point defines a gradient strength to be 27.0 mT/m, the second constraint point specifies a +10% linearity of the gradient field along the gradient (x) axis and up to the distance of 26.5 cm for the isocentre of the gradient field, while the third constraint point specifies a -20% uniformity of the gradient field inside the 40 cm imaging volume.

[0038] With the presence of these constraints on Tables 1 and 2, and the application of the inverse approach meth-

BNSDOCID: <EP___1094330A2_I_>

odology of Figure 4, the values for the Fourier coefficients for the current density of the shielded x and y-gradient coils are generated. Applying the Stream Function technique to the continuous current densities for both transverse shielded coils, the discrete current patterns for these coils were generated. Specifically, the x-gradient coil, the Stream Function technique generates 23 discrete loops on one quadrant of the primary coil, as shown in FIGURE 5A and 11 loops on one quadrant of the single shield, as shown in FIGURE 5B. The common current per loop is 376.99 amps. In this case, the eddy current from the discrete coil configuration is 0.245% over a 50 cm DSV.

[0039] By discretizing the current density for the y-gradient coil, the current density for one quadrant of the exemplary primary coil is approximated by 23 loops with a common current of 375.11 amps, as shown in FIGURE 6A, while the one quadrant of the shielding coil can be approximated by 10 loops carrying the same current per loop (FIGURE 6B). For the y-gradient coil, the eddy currents are only 0.257%. Employing the Biot-Savart law to the discrete current densities for both the x- and y shielded gradient coils, the gradient magnetic field for both of these coils is evaluated along the perspective gradient axis and at the $z = 0.0$ plane. The behavior of the gradient magnetic field for the x-gradient coil again is substantially as illustrated in FIGURE 3.

[0040] The behavior of the gradient magnetic field for the y-gradient coil is substantially as shown in FIGURE 3. Table 3 illustrates the magnetic properties for the x and y shielded gradient coils in more specific detail with a single shield.

Properties	x-gradient coil	y-gradient coil
Gradient Strength (mT/m)	27	27
Gradient Linearity (ρ = ±22.5 cm)	0.8%	7.8%
Gradient Uniformity (z = ±20.0 cm)	-20%	-20%
Rise Time @ 700V	465 μsec	442 μsec
Slew Rate @ 700V	60 T/m/sec	61 T/m/sec
% Eddy Current on 50 cm DSV	0.245%	0.257%

Table 3: Gradient field characteristics for the shielded x and y-gradient coils.

[0041] Initially, the design of the finite shielded axial z-gradient coil involves the design of the primary coil (the coil that is closest to the subject) based on the inverse approach methodology. For z-gradient coil, the gradient magnetic field is anti-symmetric in the z direction around the geometric centre of the coil, while it is symmetric along the x and y directions. Thus, in this case there is no azimuthal dependance on the current density. To generate such a field, the analytical expression of the current for the primary coil $J^a(r)$ can be written as:

$$\vec{J}^a(\vec{r}) = j_\varphi^a(z)\hat{a}_\varphi\delta(\rho - a) \tag{13}$$

where $\delta(\rho-a)$ is the restriction that the current is confined on the cylindrical surface with radius a. The restriction to inner coil length, the confinement of the current density on the cylindrical surface, the azimuthal and axial symmetries for the j^a_φ and the constraint that the current density obeys the continuity equation provides the Fourier series expansion for both components around the geometric centre of the coil as follows:

$$j_\varphi^a(z) = \sum_{n=1}^{\infty} j_{\varphi n}^a \sin(k_n z) \qquad \text{for} \qquad |z| \le \frac{L_a}{2} \tag{14}$$

BNSDOCID: <EP___1094330A2_I_>

where $j^a_{\varphi n}$ are the Fourier coefficients, L_a represents the total length of the inner coil, and $k_n=(2n\pi)/L_a$ since the current does not flow off of the ends of the cylinder. Furthermore, the current component is zero for $|z|>L_a/2$.

[0042] In order to minimize the fringe field of the primary coil in the area which is outside both the primary and the shielding coil, the Fourier transform of the current for the shielding coil satisfies the following relationship:

$$j_\varphi^b(k)=-\frac{aI_1(ka)}{bI_1(kb)}\,j_\varphi^a(k) \tag{15}$$

with

$$j_\varphi^a(k)=\frac{iL_a}{2}\sum_{n=1}^{\infty} j_{\varphi_n}^a \psi_n(k)$$

$$\psi_n(k)=\left[\frac{-\sin(k-k_n)\frac{L_a}{2}}{(k-k_n)\frac{L_a}{2}}+\frac{\sin(k+k_n)\frac{L_a}{2}}{(k+k_n)\frac{L_a}{2}}\right] \tag{16}$$

where I_m, K_m represent the derivatives with respect to the argument of the modified Bessel functions of the first and second kind.

[0043] In this case, the expression for the z component of the magnetic field B_z in the area inside both coils can be written as:

$$B_z=-\frac{\mu_0 aL_a}{2\pi}\sum_{n=1}^{\infty} j_{\varphi n}^a \int_0^{+\infty} dk\, k\, \sin(kz)\psi_n(k)I_0(k\rho)K_1(ka)\left[1-\frac{I_1(ka)K_1(kb)}{I_1(kb)K_1(ka)}\right] \tag{17}$$

[0044] Furthermore, the expression for the stored magnetic energy W can also be written as:

$$W=\frac{\mu_0 a^2 L_a^2}{4}\sum_{n=1}^{\infty}\sum_{n'=1}^{\infty} j_{\varphi_n}^a j_{\varphi_n'}^a \int_0^{+\infty} dk\;\psi_n(k)\psi_{n'}(k)I_1(ka)K_1(ka)\left[1-\frac{I_1(ka)K_1(kb)}{I_1(kb)K_1(ka)}\right] \tag{18}$$

[0045] As a next step, we construct the functional ε in terms of W and B_z as

$$\varepsilon(j_{\varphi_n}^a)=W-\sum_{j=1}^{N}\lambda_j\left(B_z(\vec{r}_j)-B_{zSC}(\vec{r}_j)\right) \tag{18a}$$

where λ_j are the Lagrange multipliers and B_{zSC} represent the constraint values of the z component of the magnetic field at the specified N points. Minimizing ε, a quadratic function of the current, with respect to the current coefficients $j^a_{\varphi n}$, results in a matrix equation which $j^a_{\varphi n}$, satisfies:

BNSDOCID <EP_ 1094330A2 I >

$$\sum_{n'=1}^{\infty} j^{a}_{\varphi_n'}(aL_a\pi)\int_0^{+\infty} dk\psi_n(k)\psi_{n'}(k)I_1(ka)K_1(ka)\left[1-\frac{I_1(ka)K_1(kb)}{I_1(kb)K_1(ka)}\right]$$
$$=-\sum_{j=1}^{N}\int_0^{+\infty} dk\ k\ \sin(kz_j)\psi_n(k)I_0(k\rho_j)K_1(ka)$$
$$\left[1-\frac{I_1(ka)K_1(kb)}{I_1(kb)K_1(ka)}\right] \qquad (19)$$

where the evaluation of the Lagrange multipliers λ_j can be done via the constraint equation.

[0046] By truncating the previous infinite summations at M terms, and using compact notation, the previous expression is modified to read:

$$\sum_{n'=1}^{M} j^{a}_{\varphi_n'} C_{n',n} = \sum_{j=1}^{N} \lambda_j D_{jn} \qquad (20)$$

or in matrix form:

$$J^a C = \lambda D \Rightarrow J^a = \lambda D C^{-1} \qquad (21)$$

but,

$$B_z = J^a D^t \Rightarrow B_z = \lambda D C^{-1} D^t \qquad (22)$$

which leads to

$$\lambda = B_z[DC^{-1}D^t]^{-1} \Rightarrow J^a = B_z[DC^{-1}D^t]^{-1}DC^{-1} \qquad (23).$$

[0047] Inverting the previous matrix equation, a solution for $j^a_{\varphi n}$, and hence for the current density, is obtained. When the continuous current distribution for both the primary and shield coils J^a, J^b is evaluated, the application of the centre of mass technique yields the discrete loop patterns for both primary and shield coils with the extra constraint that the absolute integer number of turns for both coils for a given common current value per loop is obtained. The discretization and the magnetic gradient field inside the desired imaging volume are then calculated proceeding with steps 6 through 8 of Figure 4.

[0048] Similar design procedures are followed for the exemplary axial gradient coil. In this case the radius of the cylinder for the first primary coil is set equal to 0.356000 m and its total length is set to 1.050 m. In addition, the radius of the secondary coil is equal to 0.424929 m. For the design of the primary coil the constraints are shown in Table 4.

BNSDOCID: <EP___1094330A2_I_>

n	ρ_i	z_i	B_{zSC} (T)
1	0.0000	0.001	0.000025000
2	0.0000	0.265	0.0072875000
3	0.1125	0.001	0.000025000
4	0.2250	0.001	0.000025000

Table 4: Constraint set used for the design for the shielded z-gradient coil.

Values for ρ and z are in m, values for B_{zSC} (T) are in Tesla.

[0049] As shown in Table 4, the first constraint point defines a gradient strength for the primary and shield coil to be 25.0 mT/m, the second constraint point specifies a +10% linearity of the gradient field along the gradient (z) axis and up to the distance of 26.5 cm for the isocentre of the gradient field, while the rest of the constraint points specify the uniformity of the gradient field inside the 45 cm imaging volume.

[0050] With the presence of these constraints on Table 4 and the application of the inverse approach methodology of Figure 4, the values for the Fourier coefficients for the current density of the shielded z-gradient coil are generated. Applying the centre of mass technique to the continuous current densities for both the primary coil and the shielding coil, the discrete current patterns for these coils were generated. Specifically, for the preferred first primary and the shield configuration, the centre of mass technique generates 60 discrete loops on the primary coil and 30 loops on the single shield. The common current per loop is 347.388 amps. In this case, the eddy current from the discrete coil configuration is 0.19% over a 50 cm DSV. Table 5 illustrates the magnetic properties of the shielded x-gradient coil.

Properties	z-gradient coil
Gradient Strength (mT/m)	25
Gradient Linearity (ρ = ±22.5 cm)	+0.14%
Gradient Uniformity (z = ±20.0 cm)	4.56%
Rise Time @ 700V	312 μsec
Slew Rate @ 700V	80 T/m/sec
% Eddy Current on 45 cm DSV	0.19%

Table 5: Gradient field characteristics for the z-gradient coil.

BNSDOCID: <EP___1094330A2_I_>

[0051] With reference to FIGURES 7A and 7B, images of linear distortion grids are generated for the transverse orientations (x,y plane) corresponding to the x and y gradient coils for gradient fields with and without a rollover point inside the physical space defined by the inner diameter of the gradient structure. Comparing the images from gradient coils with and without a rollover point inside a 60 cm diameter sphere, both are substantially linear near the isocentre. It will be seen in FIGURE 7B, that the grid lines adjacent the image fold back and overlap each other. This severe aliasing cannot be corrected by a distortion algorithm. This is not the case in FIGURE 7A, where the gradient field does not have a rollover point inside the physical space defined by the dimensions of the gradient coil.

[0052] Rather, because the grid lines spread uniquely at the edge, it is relatively simple to map the grid back into straight lines. This same map corrects subsequent images.

[0053] Similar results are obtained in the coronal orientation (y,z plane). Compare coronal images of the grid phantom from the gradient set without a rollover point (FIGURE 8A) to the distorted grid image generated by the gradient set with an inherent rollover point (FIGURE 8B). In FIGURE 8B, the rollover point causes grid lines along the side to be compressed and indistinguishably overlap each other. By contrast, in FIGURE 8A, the image is magnified (expanded outward) along the edges keeping each grid line warped but unique. The warped but unique grid lines are readily mapped to linear.

[0054] Similar conclusions are drawn by comparing the sagittal distortion grid of a gradient set without a rollover point to the distortion grid of a gradient set with an inherent rollover point (not illustrated).

[0055] It should be appreciated that the specified current patterns can be changed to produce either better linearity at the price of coil efficiency, and/ or greater efficiency at the price of linearity. Further, the dimensions (radius and/or length) of the cylindrical gradient coils can be changed to be increased or decreased according to the preferred application, In addition, the lengths of the primary coils and/or the secondary coils can be similar or different.

[0056] The present invention is applicable to other alternative gradient coil geometries, such as elliptical, planar, flared, etc., as well as the asymmetric gradient coil designs or any combination thereof The present invention is also applicable to the design of gradient coil structures suitable for vertically oriented or open magnet systems. Further, the disclosed primary and screen coil set can be bunched (concentrated) or thumbprint designs generated using forward or inverse approach methods. In addition, the primary and the shield coils can have any possible mixing of bunched and/or thumbprint designs. It is contemplated that zero net thrust force or torque can be incorporated into the proposed design algorithm in a known manner.

Claims

1. Magnetic resonance imaging apparatus comprising: a main magnet **(12)** for generating a main magnetic field through and surrounding an examination region **(14)**; a gradient coil assembly **(22)** for generating gradient magnetic fields **(90)** across the examination region **(14)**, which gradient magnetic fields **(90)** have a non-zero first derivative in and adjacent the examination region **(14)**; an RF transmitter **(24)** and coil assembly **(26)** positioned adjacent the examination region **(14)** such that it excites magnetic resonance dipoles in and adjacent the examination region **(14)**; an RF coil **(26)** and receiver assembly **(30)** which receives and demodulates magnetic resonance signals from the resonating dipoles; and a reconstruction processor **(50)** for reconstructing the demodulated magnetic resonance signals into an image representation.

2. Magnetic resonance imaging apparatus as claimed in claim 1, wherein the gradient coil assembly **(22)** includes: a primary gradient coil set **(22a)** disposed adjacent the examination region **(14)**, said primary gradient coil set **(22a)** including an array of conductive loops for generating the gradient magnetic fields **(90)** along three orthogonal axes; a secondary shielding coil set **(22b)** disposed between the primary coil assembly **(22a)** and the main magnet **(12)**, said secondary shielding coil set **(22b)** including an array of conductive loops such that a current density flowing thereon causes a magnetic flux density which interacts with a magnetic flux density generated by the primary magnetic field to substantially zero a net magnetization flux density outside an area defined by the secondary shielding coil set **(22b)**.

3. Magnetic resonance imaging apparatus as claimed in claim 2, wherein the primary gradient coil set **(22a)** and secondary shielding coil set **(22b)** are arranged on formers **(60, 70)**.

4. Magnetic resonance imaging apparatus as claimed in claim 3, wherein the formers **(60, 70)** are hollow cylindrical tubes arranged such that the examination region **(14)** is defined inside the former **(60)** of the primary gradient coil set **(22a)** with the former **(60)** of the primary gradient coil set **(22a)** positioned inside the former **(70)** of the secondary, shielding coil set **(22b)**.

BNSDOCID: <EP___1094330A2_I_>

5. Magnetic resonance imaging apparatus as claimed in any one of claims 1 to 4, wherein the gradient magnetic field **(90)** generated along at least one axis has (i) a substantially constant slope along a central region of the examination region **(14)** and (ii) an increasingly steep slope adjacent edges of the examination region **(14)**.

6. Magnetic resonance imaging apparatus as claimed in claim 5 further including: a linearity correction processor **(52)** which adjusts at least one of the demodulated resonance signals and the image representation to correct for distortion attributable to the increasingly steep slope of the gradient magnetic field **(90)** adjacent edges of the examination region **(14)**.

7. Magnetic resonance imaging apparatus as claimed in any one of claims 1 to 6, wherein the gradient coil assembly **(22)** includes three primary gradient coil sets **(62, 66, 68)**, one for generating a gradient magnetic field along each of three orthogonal axes, each of the primary gradient coil sets **(62, 66, 68)** generating a corresponding gradient magnetic field **(90)** which is linear adjacent a central region of the examination region **(14)** and monotonically increasing adjacent edges of the examination region **(14)**.

8. A method of designing a gradient coil assembly **(22)** for magnetic resonance imaging systems, the method comprising:

(a) selecting radius and length **(100, 102)** for a primary gradient coil set **(22a)** and radius and length for a secondary, shielding coil set **(22b)**;

(b) generating a first continuous current distribution **(106)** for the primary gradient coil set **(22a)** such that the first continuous current distribution is confined within predetermined finite geometric boundaries of a first surface defined in step (a), said first continuous current distribution generating a gradient magnetic field **(90)** across an examination region **(14)** whose first derivative in and adjacent the examination region **(14)** is non-zero;

(c) generating a second continuous current distribution **(108)** for the secondary, shielding coil set **(22b)** such that the second continuous current distribution is confined within the predetermined finite geometric boundaries defined in step (a), the first and second continuous current distributions generating a magnetic field which substantially cancels in an area outside a region defined by the secondary, shielding coil set **(22b)**;

(d) optimizing **(104)** the primary gradient coil set **(22a)** with the secondary, shielding coil set **(22b)** utilizing an energy/inductance minimization algorithm; and

(e) discretizing **(110)** the primary gradient coil set **(22a)** and the secondary, shielding coil set **(22b)**.

9. A method as claimed in claim 8, wherein the method further comprises:

(f) applying the Biot-Savart law **(112)** to the discrete current pattern to verify its validity; and
(g) measuring and mapping non-linearities **(114)** present in one of (i) the gradient magnetic field near edges of the examination region and (ii) edges of magnetic resonance images of a subject extending substantially to the edges (FIGS. 7A, 8A) of the examination region **(14)** in order to generate a correction map **(52)**.

10. A shielded gradient coil assembly **(22)** designed by the method of claim 8 or claim 9.

BNSDOCID: <EP___1094330A2_I_>

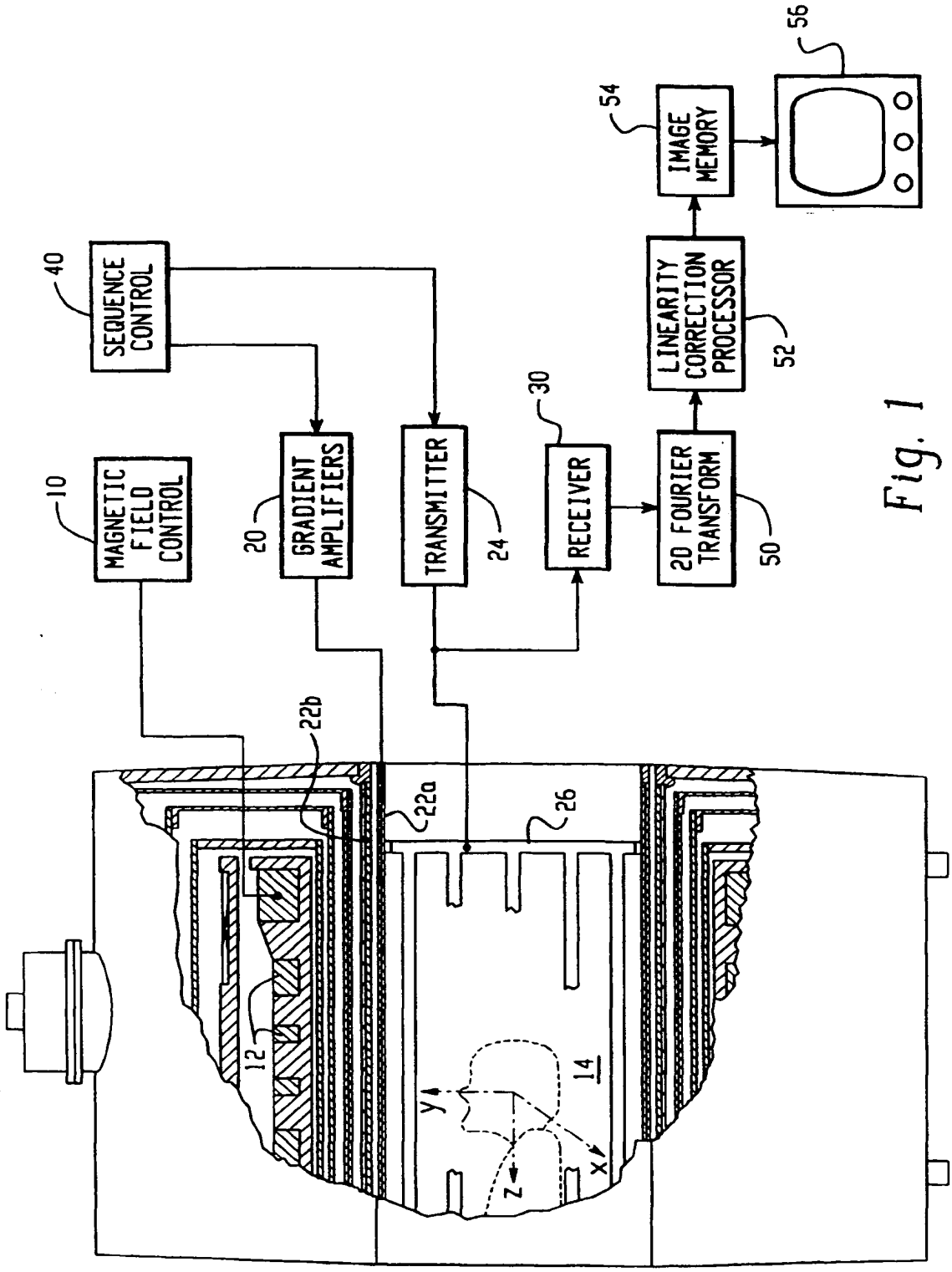

Fig. 1

BNSDOCID: <EP___1094330A2_I_>

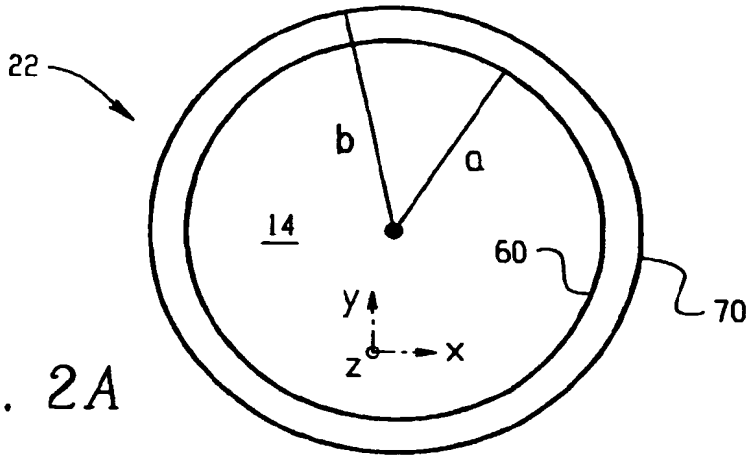

Fig. 2A

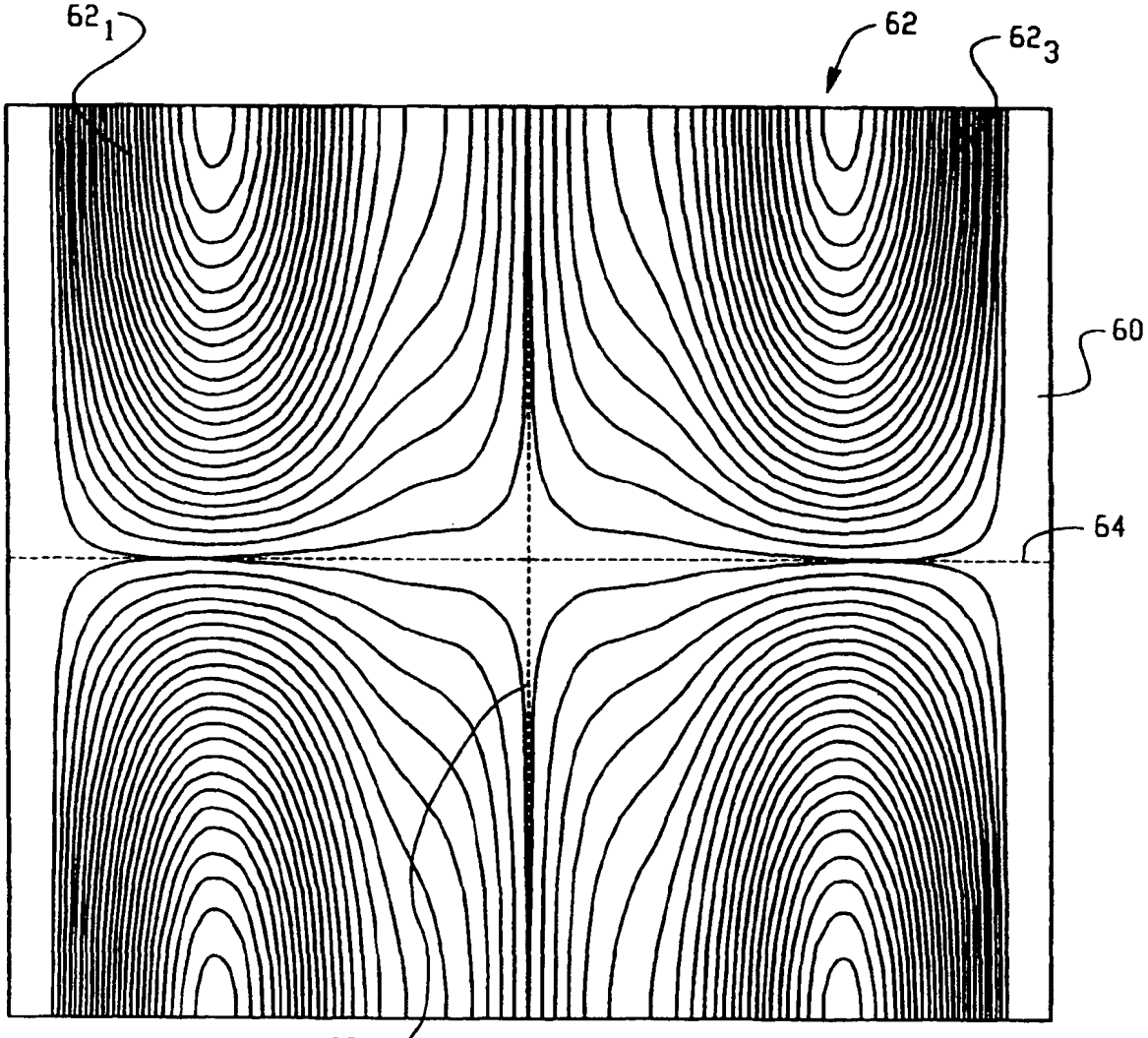

Fig. 2B

BNSDOCID: <EP___1094330A2_I_>

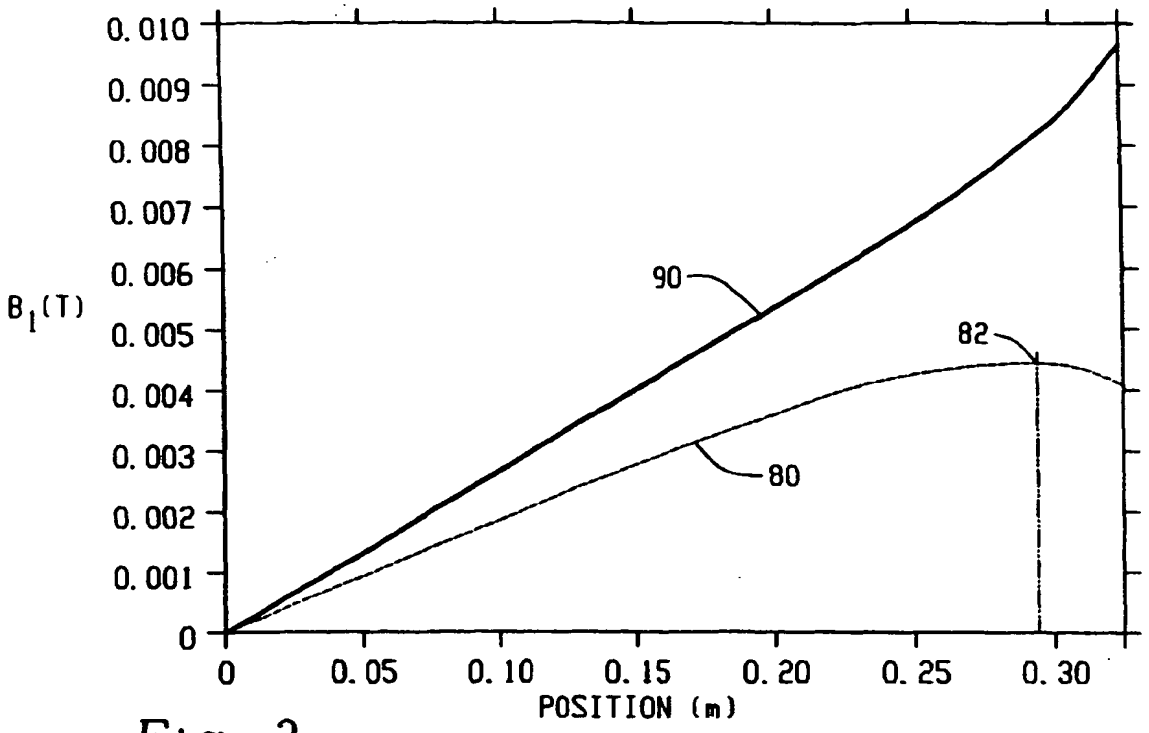

Fig. 3

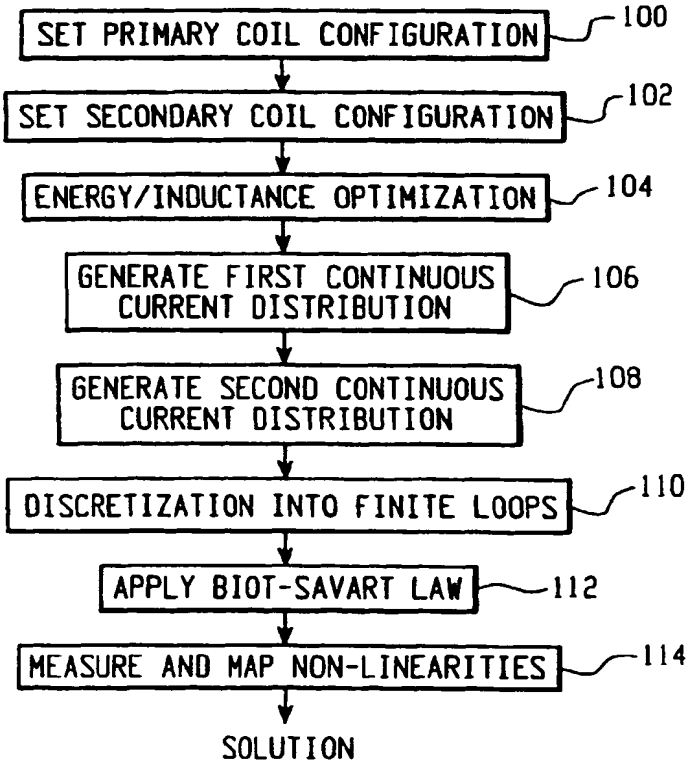

Fig. 4

BNSDOCID: <EP___1094330A2_I_>

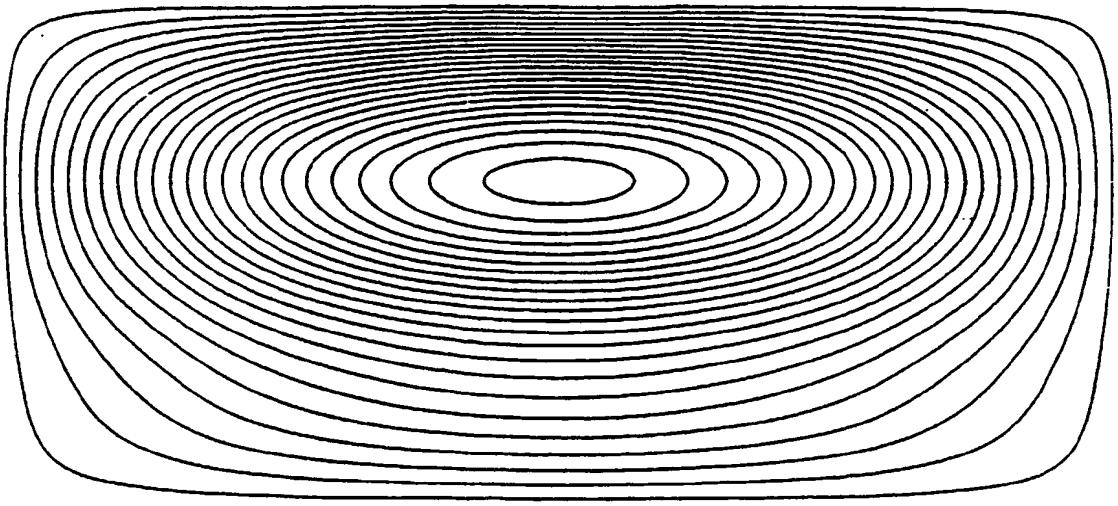

Fig. 5A

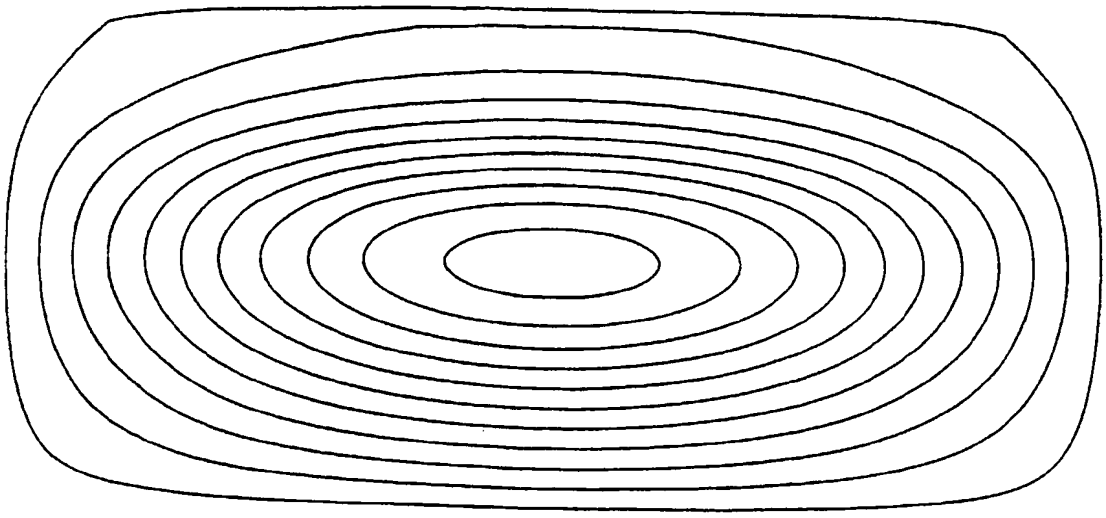

Fig. 5B

BNSDOCID: <EP___1094330A2_I_>

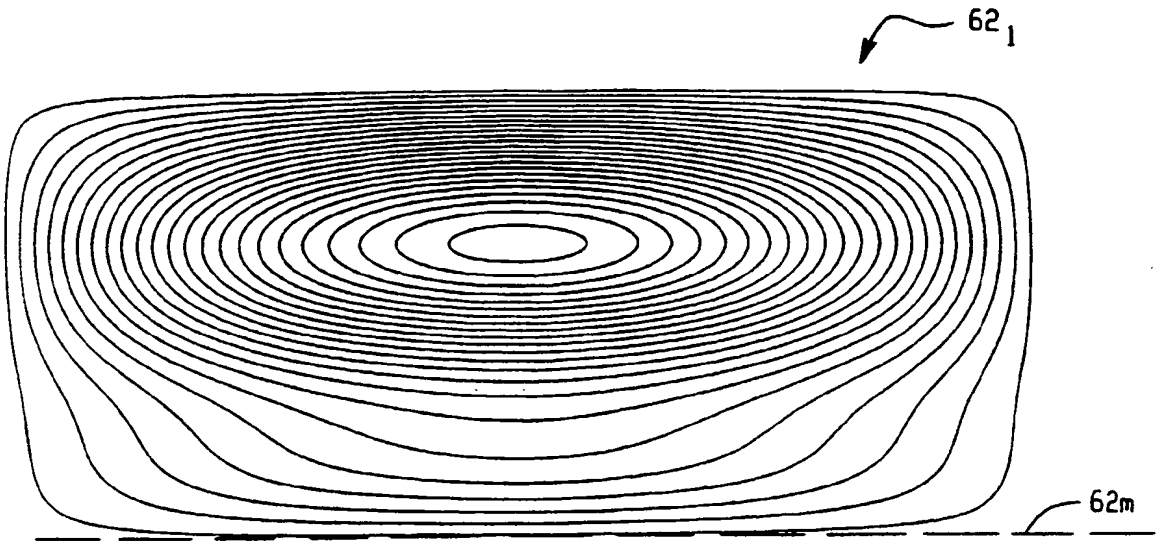

Fig. 6A

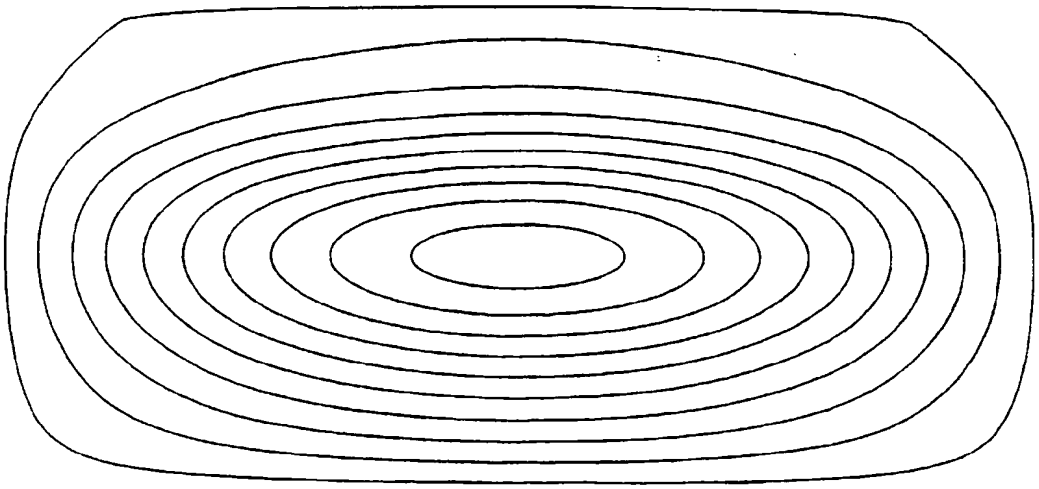

Fig. 6B

BNSDOCID: <EP__ 1094330A2_I_>

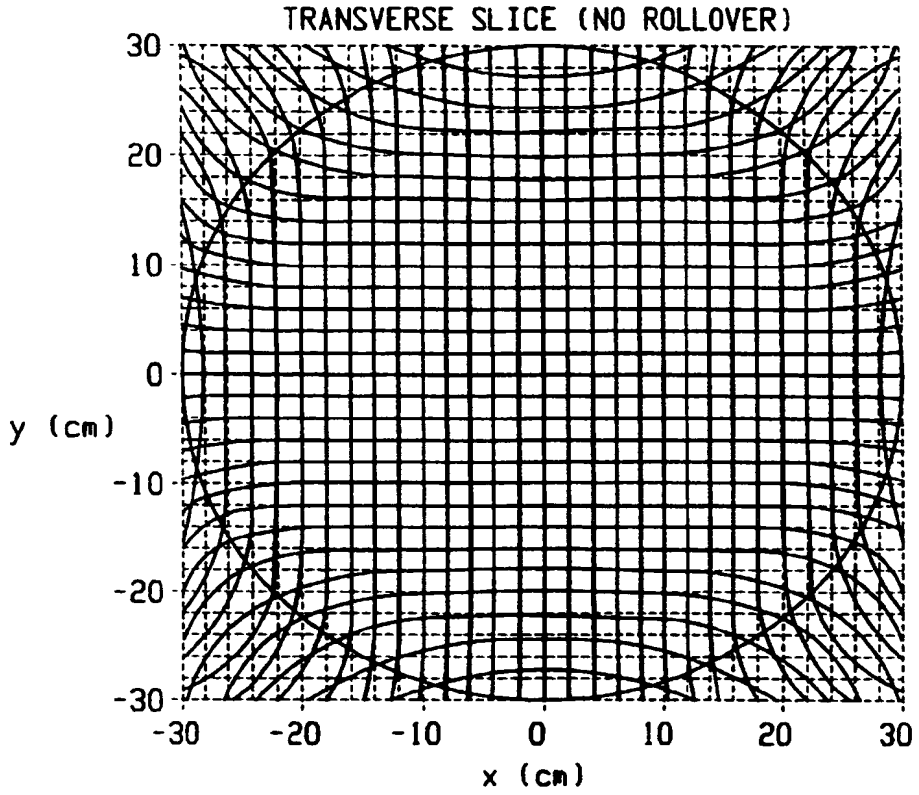

Fig. 7A

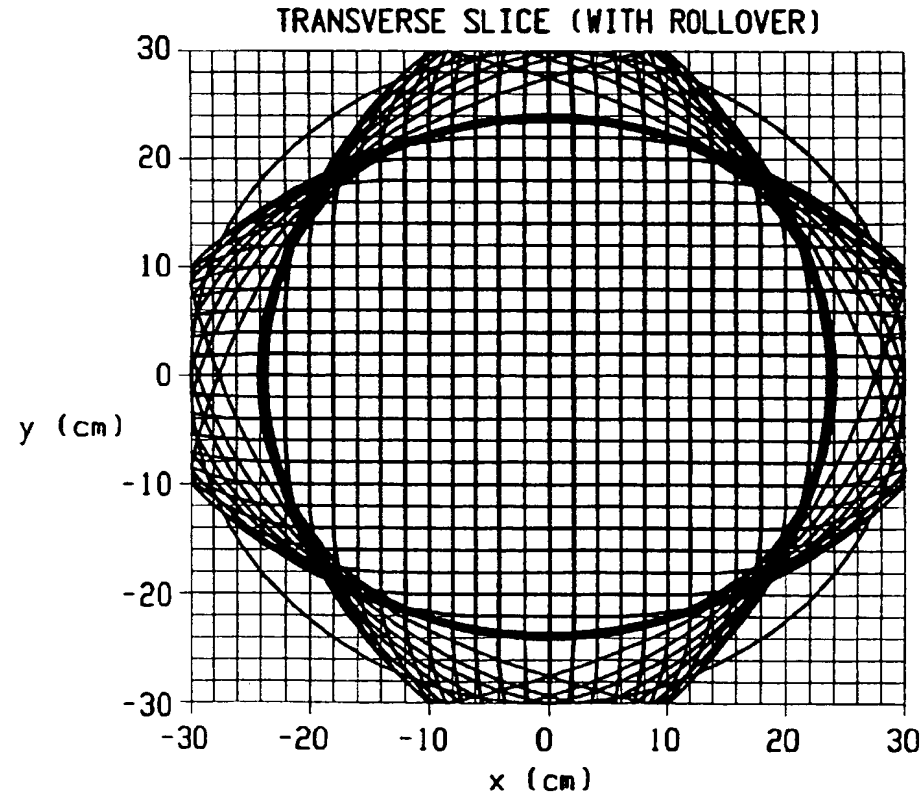

Fig. 7B
(PRIOR ART)

BNSDOCID: <EP___1094330A2_I_>

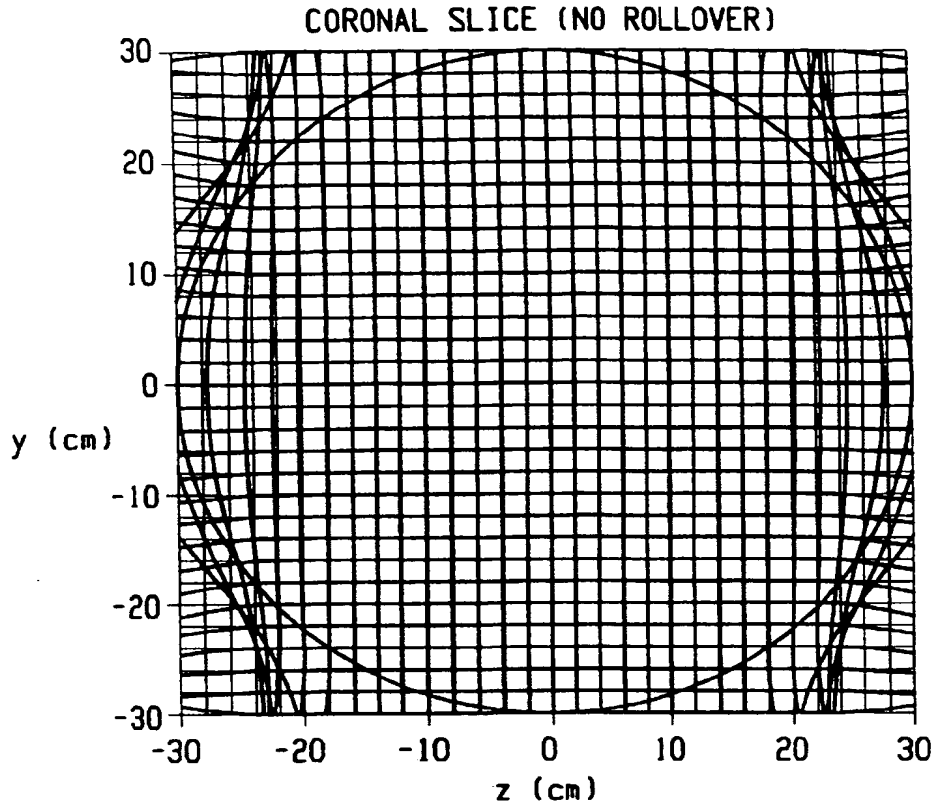

Fig. 8A

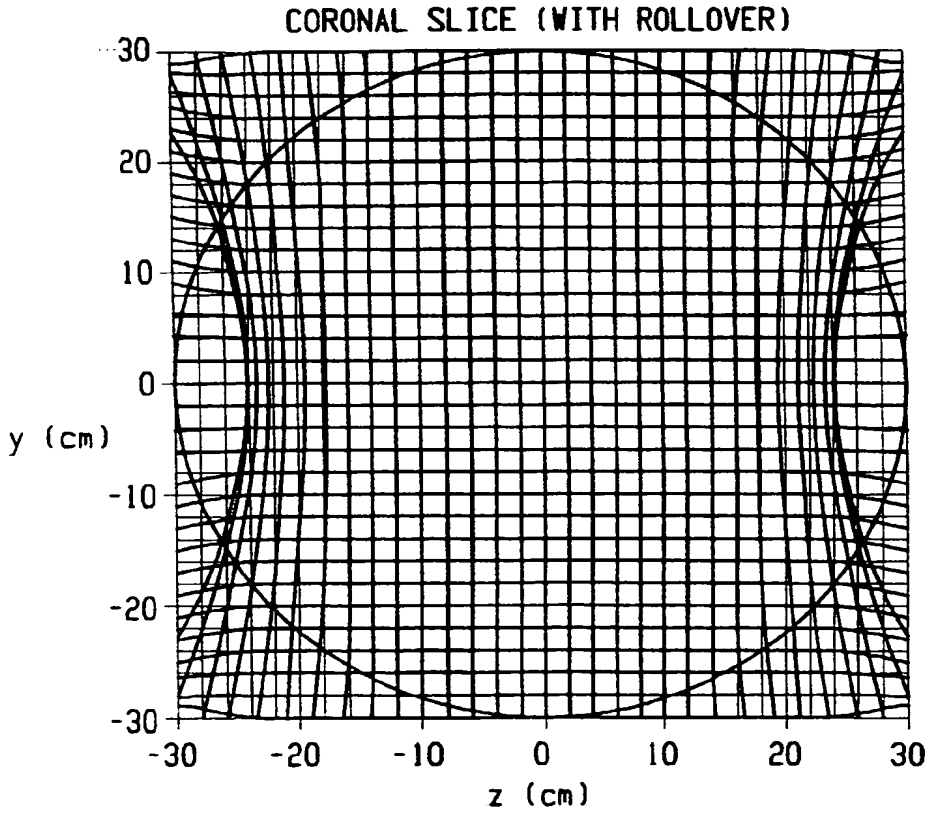

Fig. 8B
(PRIOR ART)

BNSDOCID: <EP___1094330A2_I_>

This Page Blank (uspto)